Isothermal versus non-isothermal calorimetric technique to evaluate thermokinetic parameters and thermal hazard of *tert*-butyl peroxy-2-ethyl hexanoate

Lung-Chang Tsai · Yun-Ting Tsai · Chun-Ping Lin · Shang-Hao Liu · Tsung-Chih Wu · Chi-Min Shu

Abstract Liquid organic peroxides have been broadly employed in the process industries such as *tert*-butyl peroxy-2-ethyl hexanoate (TBPO). This study investigated the thermokinetic parameters of TBPO, a typical liquid organic peroxide, by isothermal kinetic algorithms and non-isothermal kinetic algorithms with thermal activity monitor III, and differential scanning calorimetry, respectively. An attempt has been made to determine the thermokinetic parameters by simulation software, such as exothermic onset temperature (T_0), maximum temperature (T_{max}), decomposition (ΔH_d), activation energy (E_a), self-accelerating decomposition temperature, and isothermal time to maximum rate (TMR_{iso}). A liquid thermal explosion model was established for a reactor containing liquid organic peroxide of interest. From experimental results, liquid organic peroxides' optimal conditions for avoiding a violent runaway reaction of storage and transportation were created.

List of symbols

A	Frequency factor (s^{-1})
C_p	Heat capacity $(J\ g^{-1}\ K^{-1})$
E_a	Activation energy $(kJ\ mol^{-1})$
k	Thermal conductivity $(W\ m^{-1}\ K^{-1})$
k_0	Reaction rate constant (min^{-1})
k_i	Reaction rate constant at isothermal temperature $(min^{-1}, i = 0, 1, 2, 3)$
n_i	Reaction order of ith stage (dimensionless)
Q_{max}	Maximum heat flow $(W\ g^{-1})$
SADT	Self-accelerating decomposition temperature (°C)
T	Absolute temperature (K)
T_0	Exothermic onset temperature (°C)
T_e	Ambient temperature (°C)
T_f	Final temperature (°C)
T_{iso}	Isothermal temperature (°C)
T_P	Peak temperature (°C)
TMR_{iso}	Time to maximum rate under isothermal condition (h)
t	Time (s)
Z	Autocatalytic constant (dimensionless)
α_i	Degree of conversion (dimensionless)
β	Heating rate (°C min^{-1})
ΔH_d	Heat of decomposition $(J\ g^{-1})$

L.-C. Tsai
Department of Safety Engineering, School of Chemical Engineering, Nanjing University of Science and Technology, 200, Xiao Ling Wei Street, Nanjing 210094, China, PRC

Y.-T. Tsai · S.-H. Liu · C.-M. Shu (✉)
Department of Safety, Health, and Environmental Engineering, National Yunlin University of Science and Technology, 123, University Rd., Sec. 3, Douliou, Yunlin 64002, Taiwan, ROC
e-mail: shucm@yuntech.edu.tw

C.-P. Lin
Department of Health and Nutrition Biotechnology, College of Health Science, Asia University, 500, Lioufeng Rd., Wufeng, Taichung 41354, Taiwan, ROC

T.-C. Wu
Department of Safety, Health, and Environmental Engineering, Hungkuang University, 34, Chung-Chie Rd., Shalu, Taichung 43302, Taiwan, ROC

Introduction

Organic peroxides, which are substances that decompose rapidly when subjected to overheating, light exposure, pollution, friction, or mechanical impact, are widely employed in the process industries. OPs have an organic molecule attached to at least one side of the oxygen-to-oxygen bond (O–O). Their thermal instability is caused by the weak O–O bond, which leads to a tendency toward more stable condition [1]. Many OPs easily generate high pressure under exothermic situation. In general, the threshold temperature is below 120 °C, even lower than the ambient temperature [2]. The self-accelerating decomposition temperature (SADT) of OPs is recommended by the United Nations (UN) so that a precise test in a commercial package must be established [3]. SADT is the lowest ambient temperature at which over-heat in the middle of the industrial packaging exceeds 6 °C after a lapse of a seven day period or less. This period is measured every once in a while when the packaging center temperature reaches 2 °C below the surrounding temperature. The value of SADT is to precisely govern the temperature during storage and transport [4–6].

Chemical industries widely employ OPs as initiators and cross-linkers during polymerization, such as methyl ethyl ketone peroxide (MEKPO), di-*tert*-butyl peroxide (DTBP), cumene hydroperoxide (CHP), and *tert*-butyl peroxy-2-ethyl hexanoate (TBPO) [7]. We focused on major analysis of the thermal hazard characteristics for TBPO, which is particularly sensitive to temperature rises and pollution. It is generally stored or transported with inert solids to ease or mitigate the thermal hazard. TBPO reacts quite seriously when rapidly heated to a critical temperature. Several explosions were due to thermal source, mechanical shock, or friction owing to self-accelerating exothermic decomposition, or mixing with amines or certain metals can also cause accelerated decomposition [8–11].

Thermal decomposition of TBPO was examined using a thermal dynamic calorimeter (differential scanning calorimetry, DSC) and isothermal microcalorimeter (thermal activity monitor III, TAM III) to evaluate basic exothermic decomposition and various thermokinetic parameters. Furthermore, calorimetry technology was used to observe the exothermic behaviors by DSC, such as exothermic onset temperature (T_0), peak temperature (T_p), and heat of decomposition (ΔH_d), and then TAM III was used to obtain the thermokinetic parameters, such as time to maximum rate under isothermal condition (TMR$_{iso}$), and calculate E_a (activation energy) under isothermal condition and A (frequency factor) by the Arrhenius law. Based upon the above mentioned, the thermal hazard appearance for a specific chemical process can be more completely expressed.

Finally, a test platform was conducted to evaluate the thermal runaway parameters of the chemical product, in order to reduce the necessity of large-scale explosive experiments. The method can be employed in many different fields, such as evaluation of chemical process risk, reactor container design, safety of storage and transportation, and thermal hazard characteristic assessment [12].

Experimental and method

Sample

Ninety-seven mass% TBPO, a colorless liquid was packaged in the 100 mL plastic container. It was stored in a refrigerator below 4 °C.

Differential scanning calorimetry (DSC)

The DSC was purchased from Mettler, model TA8000 system DSC821^e. It is a useful tool for identifying a substance's rudimentary thermal decomposition situation quickly and clearly, and only small amount of sample is available. The principle of DSC is to compare the energy difference between the two test cells in which one sample is put in, and the other one acts a reference at different heating or cooling rates. The thermal analysis software STAR^e for DSC data was adopted to obtain heat flow curves and calculate thermokinetic parameters. The experimental test sample used was ca. 5–6 mg, and the heating rate (β) was set at 0.5, 1, 2, 3, 4, and 10 °C min^{-1} [13].

Thermal activity monitor III (TAM III)

TAM III, an isothermal titration calorimeter, which possesses high thermal sensitivity and stability, was purchased from TA Instrument. TAM III can predict many potential process risks, such as runaway reactions, temperature dependence on the decomposition of unstable substance, and safe storage condition. It can insure the life cycle of a substance after storage, and TAM Assistant can be used to evaluate a substance's exothermic reaction. It can govern the temperature range, which is 15–150 °C. As planned, the temperature of the study was 50, 60, 70, and 80 °C. The test cell was a 20 mL ampoule coupled with a glass container and aluminum lid, and 100 mg TBPO was added in the TAM III test [14].

Reaction kinetic model simulation

The thermal safety software (TSS) could facilitate our determination of the practical condition in industrial processes and evaluate from the small-scale to match the commercial scale [15]. The method was applied to the

thermal explosion model, which requires heat capacity (C_p) and thermal conductivity (k), along with an appropriate algorithm. The experimental setup simulated what the TBPO is set in a storage container that has a shell thickness of 0.1 m. The reactor had the following properties: $C_p = 1{,}800$ J g^{-1} K^{-1}, and $k = 0.5$ W m^{-1} K^{-1} [16, 17].

Results and discussion

DSC tests

Table 1 indicates the thermal decomposition of TBPB at different heating rates of 0.5, 1, 2, 3, 4, and 10 °C min^{-1}, corresponding to T_0, T_f, T_p, and ΔH_d of 74.47–105.46 °C, 118.20–155.71 °C, 97.13–134.67 °C, and 831.41–991.91 J g^{-1}. Figure 1 shows the results that the higher heating rate caused the higher exothermic peak. Therefore, it could be demonstrated that as the heating rate is increased, the exothermic peak will also be rising, because a higher heating rate provides higher intensities of the energy within a unit of time for the decomposition of TBPO. The ΔH_d was evaluated for other thermal hazard parameters for TBPO. However, the results lacked significant alternation when the heating rate increased. As mentioned above, the DSC test could be obtained at initial condition when TBPO was decomposed after continued heating. In addition, the TAM III test isothermal temperature set range could also be judged from the DSC test.

TAM III tests

In the case of isothermal temperature, regarding thermal analysis, such as innate thermal hazard of the reactants, material transport, and medicine storage, Fig. 2 shows the results of four isothermal temperatures, 50, 60, 70, and 80 °C, with TBPO [18, 19]. It indicates the exothermic peak is higher and steeper with increased temperature. In addition, according to the experimental results, TBPO did not visibly incur any prominent reaction at 50–60 °C. Therefore, caution must be taken during storage and transportation when the temperature is over 60 °C. Table 2

Table 1 Calorimetric data for the decomposition of TBPO obtained from DSC

β/°C min^{-1}	T_0/°C	T_p/°C	T_f/°C	ΔH_d/J g^{-1}
0.5	74.47	97.13	118.20	837.88
1	80.99	105.63	122.41	887.83
2	85.41	113.10	130.65	856.31
3	91.15	116.83	135.05	991.91
4	93.72	121.57	139.27	831.41
10	105.46	134.67	155.71	925.02

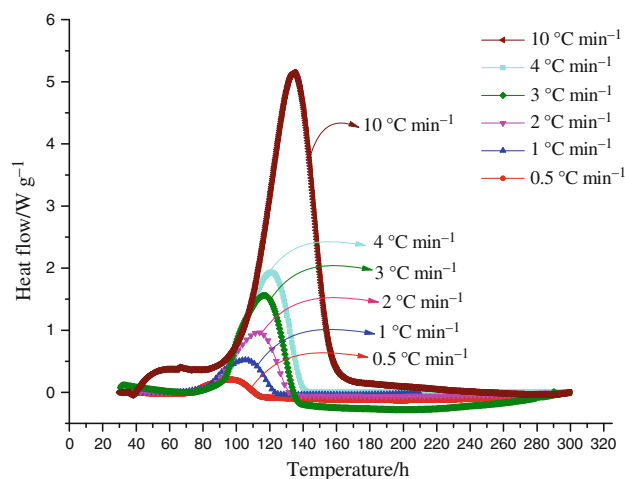**Fig. 1** DSC thermal curves of heat flow versus temperature for TBPO decomposition at heating rates of 0.5, 1, 2, 3, 4, and 10 °C min^{-1}
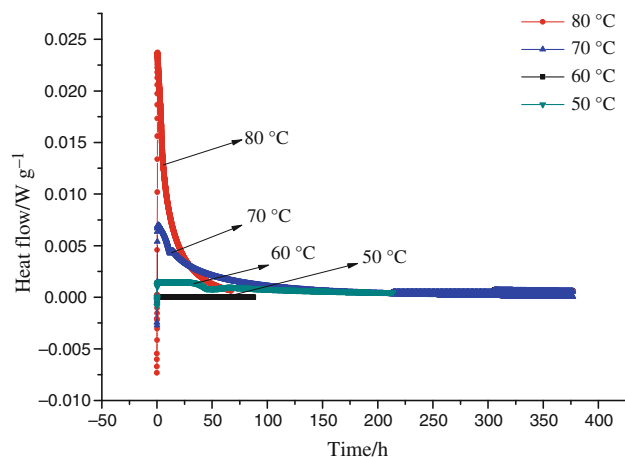

Fig. 2 TAM III thermal curves of heat flow versus time for TBPO decomposition at 50, 60, 70, and 80 °C

Table 2 Scanning data of the thermal runaway decomposition by TAM III

T_{iso}/°C	Mass/mg	TMR$_{iso}$/h	Q_{max}/W g^{-1}
50	99.2	5.951818	0.00149
60	100.1	3.926617	0.00568
70	99.6	0.456837	0.02354
80	100.1	0.491195	0.07637

shows the relationship between temperature and exothermic reaction [18]. The parameter, which is an important index for thermal hazard, is TMR$_{iso}$.

TMR$_{iso}$ indicates how much time the heat flow achieved a maximum value during an exothermic reaction. This
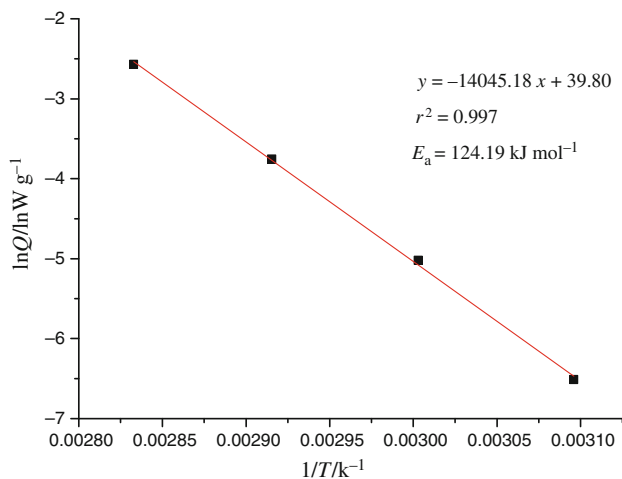
Fig. 3 Arrhenius plot for the decomposition of TBPO

Table 3 Thermokinetic parameters evaluated by nth-order simulation

T_{iso}/°C	$\ln k/\ln$ s	E_a/kJ mol^{-1}	n_1
50	44.0382	151.8369	0.7912
60	44.1021	155.8197	1.6605
70	44.0159	156.3249	1.1393
80	43.7261	157.1915	1.1585

Table 4 Thermokinetic parameters evaluated by autocatalytic simulation

T_{iso}/°C	$\ln k/\ln$ s	E_a/kJ mol^{-1}	n_1	n_2
50	26.58	104.5	0.5967	2.7812×10^{-6}
60	34.52	129.2	2.0187	2.2088
70	42.48	151.8	1.2460	2.2283×10^{-8}
80	48.05	165.7	2.1722	1.4164

information could be obtained from a diagram of heat flow versus time by TAM III [20]. In practice, TMR$_{iso}$ is determined to time the emergency response [21]. If the TMR$_{iso}$ is lower, the emergency response indicates the situation is more dangerous. Therefore, it is quite useful to emphasize chemical process safety. The results about TMR$_{iso}$ are given in Table 2.

To evaluate more clearly the thermal hazard, the various thermal hazard parameters must be obtained by specific thermokinetic model. The Arrhenius equation under isothermal condition is used to calculate activation energy and frequency factor. Equation (1) is expressed as follows:

$$k = A e^{-E_a/RT} \tag{1}$$

Equation (1) is computed with natural logarithm, with respect to four ambient temperatures. Then, Eq. (2) can be obtained:

$$\ln\left(\frac{k_2}{k_1}\right) = \frac{E_a}{R}\left(\frac{1}{T_1} - \frac{1}{T_2}\right) \tag{2}$$

As the reactant's rate constant is proportional to maximum heat flow, Eq. (2) could be changed to Eq. (3):

$$\ln\left(\frac{Q_2}{Q_1}\right) = \frac{E_a}{R}\left(\frac{1}{T_1} - \frac{1}{T_2}\right) \tag{3}$$

The plot of $\ln Q$ versus $1/T$ graph was used to determine the slope, which is equal to E_a, and the intercept is A. Therefore, the values of E_a and A are 124.19 kJ mol^{-1} and 1.9291×10^{17} s^{-1}, respectively. The results are shown in Fig. 3. The experimental results were comparable to those obtained in previous studies [22, 23].

Results of TSS simulation

Tables 3 and 4 show that, by TSS with nth-order or autocatalytic equations, TBPO's thermokinetic parameters

could be judged under the isothermal temperature. Nth-order and autocatalytic equations were applied by TSS, as displayed by Eqs. (4) and (5), respectively [24].

$$\frac{d\alpha}{dt} = k_0 e^{-E_a/RT}(1-\alpha)^n \tag{4}$$

$$\frac{d\alpha}{dt} = k_0 e^{-E_a/RT}(1-\alpha)^{n1}(z + \alpha^{n2}) \tag{5}$$

Compared with Tables 3 and 4, from the result of autocatalytic simulation it was found that the E_a value matched the result of experimental value better than nth-order reaction. Thus, TBPO decomposition is identified as an autocatalytic reaction. Figures 4, 5, 6, and 7 show the fitted curves of autocatalytic reaction under isothermal temperature of 50, 60, 70, and 80 °C by experiments and simulations. For 50 °C simulation, the results do not match
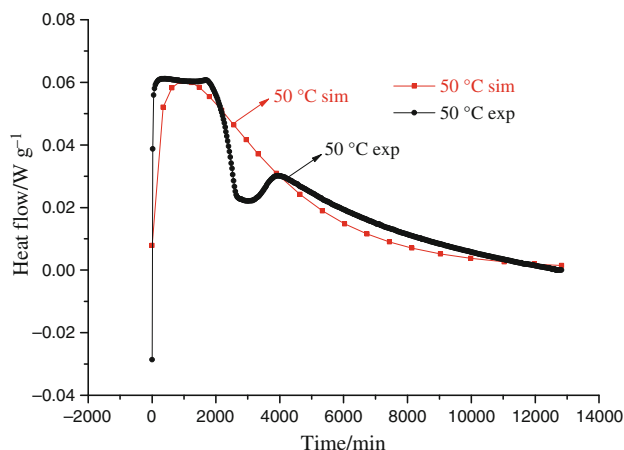

Fig. 4 Comparison of experimental and simulation results for the autocatalytic decomposition of TBPO at 50 °C
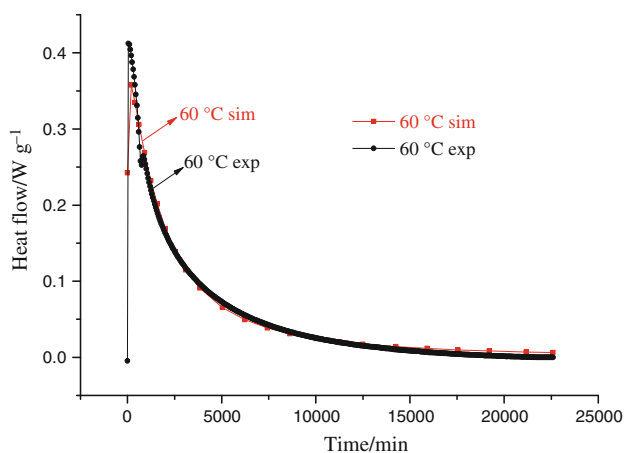
Fig. 5 Comparison of experimental and simulation results for the autocatalytic decomposition of TBPO at 60 °C
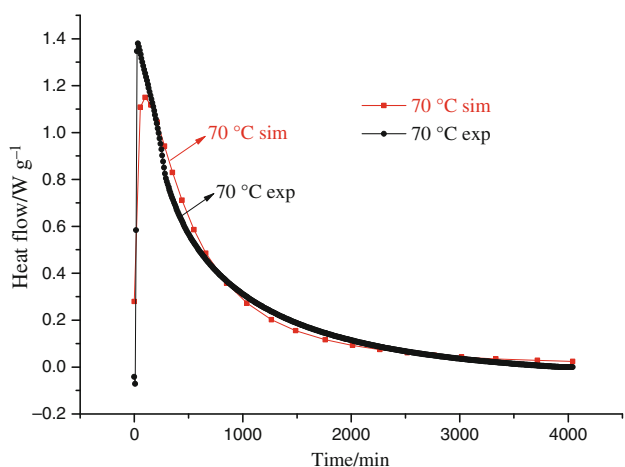

Fig. 6 Comparison of experimental and simulation results for the autocatalytic decomposition of TBPO at 70 °C
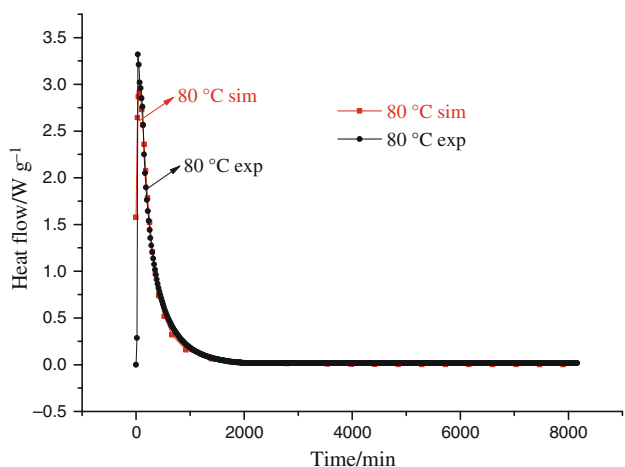

Fig. 7 Comparison of experimental and simulation results for the autocatalytic decomposition of TBPO at 80 °C

the experimental curve, which shows a different phenomenon from other temperature such as 60, 70, and 80 °C. Nevertheless, simulation results are acceptable in agreement with experimental results. TSS simulation data offered in this study demonstrated that the predicted TBPO's exothermic features had a remarkable effect.

Conclusions

A new research on runaway reactions on TBPO 97 mass% was accomplished by DSC and TAM III, which identified the related thermokinetic and safety parameters, such as ΔH_d, T_0, E_a, A, and TMR_{iso}. E_a was computed by the Arrhenius model and the results are in good agreement with those of previous studies. On the other hand, for TBPO's storage and transportation temperature, according to experimental results, the TMR_{iso} value is 0.456831 h at 70 °C, which is far less than the value of TMR_{iso} 3.926617 h at 60 °C. Thus, the chemical process control temperature of TBPO should be maintained below 60 °C. Furthermore, the result is valuable when a chemical process encounters runaway reaction to establish how much time the treatment of the emergency response has. The TSS simulation reports have exemplified that the technology can be practically applied and presents proper results.

DSC non-isothermal test and TAM III isothermal test were used to obtain various available thermokinetic and safety parameters for TBPO's safety management by calorimetric analysis technology. Moreover, we used a thermokinetic model combined with experimental data, which can predict more useful information, such as TMR_{iso}, E_a, or reaction order, to overcome the limitations of conventional thermal analysis method and to establish a safer process design.

In the future, the extended study may emphasize the TBPO mixed with specific incompatible inorganic acids, such as HCl, H_2SO_4, HNO_3, or H_3PO_4. The incompatibility could be used to evaluate the thermal hazard and explosion, after runaway excursion. Furthermore, product analysis technology could be used, such as TGA/IR/GC/MS, to thoroughly explore the decomposition mechanism for process during upsets.

References

1. Lu KT, Chen TC, Hu KH. Investigation of the decomposition reaction and dust explosion characteristics of crystalline benzoyl peroxides. J Hazard Mater. 2010;161:246–56.
2. Luo KM, Chang JG, Lin SH, Chang CT, Yeh TF, Hu KH, Kao CS. The criterion of critical runaway and stable temperatures in

cumene hydroperoxide reaction. J Loss Prev Proc Ind. 2001;14: 229–39.

3. United Nations, Committee of Experts on the Transport of Dangerous Goods, 14th Revised Ed., USA. 2005;205.

4. Fisher HG, Goetz DD. Determination of self–accelerating decomposition temperatures for self–reactive substances. J Loss Prev Proc Ind. 1993;6:183–94.

5. Fauske HK. Gassy system vent sizing the role of two-phase flow. Process Safety News. Burr Bidge, IL: Fauske and Associates, LLC; 2011;18:3.

6. AKTS AG, AKTS–Thermokinetics Software and AKTS–Thermal Safety Software. http://www.akts.com.

7. Material Safety Data Sheet. Akzo Nobel Chemicals bv Stationsplein, 4. P.O. Box 247, 3800 AE Amersfoort, The Netherlands; 2007.

8. Wu LK, Chen KY, Cheng SY, Lee BS, Shu CM. Thermal decomposition of hydrogen peroxide in the presence of sulfuric acid. J Therm Anal Calorim. 2008;93:115–20.

9. Hou HY, Duh YS, Lin WH, Shu CM. Reactive incompatibility of cumene hydroperoxide mixed with alkaline solutions. J Therm Anal Calorim. 2006;85:145–50.

10. Duh YS, Wu XH, Kao CS. Hazard ratings for organic peroxides. Process Saf Prog. 2008;27:89–99.

11. Safety and handling of organic peroxides: a guide, organic peroxide producers' safety division. The Society of the Plastics Industry (SPI) Inc., Washington, DC, USA. 1999.

12. Lin CP, Chang CP, Chou YC, Shu CM. Modeling solid thermal explosion containment on reactor HNIW and HMX. J Hazard Mater. 2010;176:549–58.

13. STAR^e Software with Solaris Operating System. Operating Instructions. Toledo: Mettler Toledo; 2004.

14. Product Information. 2012. TAM III Thermostat. www.thermo metric.com.

15. Lin CP, Chang YM, Tseng JM, Shu CM. Comparisons of nth-order kinetic algorithms and kinetic model simulation on HMX by DSC tests. J Therm Anal Calorim. 2010;100:607–14.

16. Thermal safety software (TSS). St. Petersburg, Russia: ChemInform Saint-Petersburg (CISP) Ltd. http://www.cisp.spb.ru.

17. You ML, Shu CM. Further explanations of lauroyl peroxide runaway reaction by DSC tests and simulations. J Therm Anal Calorim. 2011;103:411–2.

18. Lin CP, Tseng JM. Green technology for improving process manufacturing design and storage management of organic peroxide. Chem Eng J. 2012;180:284–92.

19. Peng JJ, Wu SH, Hou HY, Lin CP, Shu CM. Thermal hazards evaluation of cumene hydroperoxide mixed with its derivatives. J Therm Anal Calorim. 2009;96:783–7.

20. Liu SH, Lin CP, Shu CM. Thermokinetic parameters and thermal hazard evaluation for three organic peroxides by DSC and TAM III. J Therm Anal Calorim. 2011;106:165–72.

21. Tseng JM, Liu MY, Chen SL, Hwang WT, Gupta JP, Shu CM. Runaway effects of nitric acid on methyl ethyl ketone peroxide by TAM III tests. J Therm Anal Calorim. 2009;96:789–93.

22. Akzo Nobel, Organic Peroxide Initiators, Product Brochure, USA. 2012.

23. Malow M, Wehrstedt KD. Prediction of the self–accelerating decomposition temperature (SADT) for liquid organic peroxides from differential scanning calorimetry (DSC) measurements. J Hazard Mater. 2005;120:21–4.

24. Lin CP, Tseng JM, Chang YM, Liu SH, Cheng YC, Shu CM. Modeling liquid thermal explosion reactor containing *tert*–butyl peroxybenzoate. J Therm Anal Calorim. 2010;102:587–95.